Performance Analysis of Uplink Massive MIMO Networks with a Finite User Density

Xuefeng Yao[ʳ], Ming Ding[‡], David López Pérez[†], Zihuai Lin[ʳ], Guoqiang Mao[ǂ‡]
[ʳ]*School of Electrical and Information Engineering, University of Sydney, Australia* {xuefeng.yao@sydney.edu.au}
[‡]*Data61, Australia* {Ming.Ding@data61.csiro.au}
[†]*Nokia Bell Labs, Ireland* {david.lopez-perez@nokia.com}
[ǂ]*School of Computing and Communication, University of Technology Sydney, Australia*

***Abstract*—In this paper, we conduct performance analysis for uplink (UL) massive multiple input and multiple output (mMIMO) networks using stochastic geometry. With the consideration of practical system assumptions, such as sophisticated path loss model incorporating both line-of-sight (LoS) and non-line-of-sight (NLoS) transmissions and a finite user equipment (UE) density, we derive the coverage probability and the area spectral efficiency (ASE) performance. In particular, we adopt a practical user association strategy (UAS) based on the smallest pathloss since we differentiate LoS and NLoS transmissions, and we consider the correlation among the positions of UEs and base stations (BSs) in realistic networks. From our simulation and analytical results, we find that the performance impacts of the probabilistic LoS/NLoS transmissions and a finite UE density on UL mMIMO networks are significant. More specifically, the coverage probability performance suffers from a moderate decrease or even a severe degradation when the UE density becomes large in sparse mMIMO networks. Moreover, our results indicate that there exists an optimal BS density to maximize the sum spectral efficiency per BS. However, the ASE performance keeps growing with network densification.**

I. Introduction

Massive multiple input and multiple output (mMIMO) is considered as one of the most important candidate technologies to meet the ever-increasing capacity demand in the years to come [1]. By exploiting its many antennas and thus degrees of freedom in the spatial domain, mMIMO can increase the per-cell and the area spectral efficiency (ASE) through spatial multiplexing. The larger the number of antennas, the larger the number of degrees of freedom, and thus the more multiplexing opportunities. However, when a time division duplex (TDD) system is considered, the performance of mMIMO may be limited by inaccurate channel state information (CSI). Pilot contamination is one of the major bottlenecks, and occurs when the same set of uplink (UL) pilot sequences is reused across neighbouring cells [2].

Up to now, most theoretical studies on mMIMO have focused on TDD systems. However, the majority of them have only considered a simple modeling with a limited number of factors. In [2], the authors derived the signal to interference ratio (SIR) distribution of both uplink and downlink using a simple network topology, and showed that increasing the number of antennas at the BS leads to a better performance. In [3], the authors derived the UL signal to interference plus noise ratio (SINR) and sum rate of the system based on deterministic BS locations. In [4], the authors analyzed the UL SINR and rate performance using stochastic geometry, and showed a scaling law between the number of antennas per BS and the number of scheduled UEs. Note that all of the above studies considered the pilot contamination. It is also important to note that all of the above studies considered a simple single-slope path loss model, without differentiating line of sight (LoS) and non-LoS (NLoS) transmissions, and a infinite (or sufficiently large) user equipment (UE) density, thus ignoring the performance impact of important system aspects on mMIMO networks.

In this paper, we conduct performance analysis of the UL TDD mMIMO networks with maximum ratio combining (MRC) receivers using stochastic geometry. We consider several practical assumptions, i.e., pilot-aided channel estimation, a multi-slope path loss model with probabilistic LoS and NLoS transmissions, and a finite UE density. Compared with the existing work, we also adopt a more practical UE association strategy (UAS) based on the largest receive signal strength. Since we differentiate between LoS and NLoS transmissions, the base station (BS) at the closest geographical distance from a UE may not be the BS at the closet radio distance. This makes our analytical results more accurate.

From our simulation and analytical results, we find that the performance impacts of the probabilistic LoS/NLoS transmissions and a finite UE density are significant. More specifically, the coverage probability performance suffers from a moderate decrease or even a severe degradation when the UE density becomes large in sparse mMIMO networks. Moreover, our results indicate that there exists an optimal BS density to maximize the sum spectral efficiency per BS. However, the ASE performance keeps growing with network densification.

II. System Model

In this section, we present the network scenario, wireless system model, pilot-aided mMIMO channel estimation and performance metrics.

A. Network Scenario

In this paper, we consider an UL cellular network with UEs deployed on a plane according to a homogeneous Poisson

point process (HPPP) Φ with a density of ρ UEs/km^2. BSs are also Poisson distributed in the considered network with a density of λ BSs/km^2. Note that we only consider active UEs in the network because non-active UEs do not trigger any data transmission, and that UEs and BSs are deployed independently. Note that a typical UE density in populated 5G scenarios is around $\rho = 300$ UEs/km^2 [5].

We assume that the typical UE U_1 is deployed at the origin and its serving BS is denoted by B_1. Each BS and each UE are equipped with M and one antennas, respectively.

In practice, a BS will enter into idle mode, if there is no UE connected to it, which reduces the interference to UEs in neighbouring BSs as well as the energy consumption of the network. Since UEs are randomly and uniformly distributed in the network, the active BSs also follow another HPPP distribution $\tilde{\Phi}$ [6], the density of which is $\tilde{\lambda}$. Note that $\tilde{\lambda} \leq \lambda$ and $\tilde{\lambda} \leq \rho$, since one UE is served by at most one BS. Also note that a larger ρ results in a larger $\tilde{\lambda}$.

From [6], $\tilde{\lambda}$ can be calculated as

$$\tilde{\lambda} = \lambda \left[1 - \frac{1}{\left(1 + \frac{\rho}{q\lambda}\right)^q} \right], \tag{1}$$

where an empirical value of 3.5 was suggested for q.

Moreover, we consider a pilot-aided channel estimation scheme, which leads to imperfect CSI caused by pilot contamination. In an UL training stage, a scheduled UE transmits a randomly assigned pilot sequence t_k from the set of available pilot sequences $\mathcal{T}$. UEs in each BS reuse the same set of pilot sequences. For each scheduled UE, the BS first detects its corresponding pilot sequence, which is transmitted from such scheduled UE and interfered by all the other UEs in neighbouring cells reusing the same pilot sequence. The BS then estimates the UE's channel by, e.g., a minimum mean square error (MMSE) estimator.

According to [7], the UE number per BS can be denoted by a random variable (RV) K, and the probability mass function (PMF) of K can be derived as

$$\begin{aligned} f_K(k) &= \Pr[K = k] \\ &= \frac{\Gamma(k+q)}{\Gamma(k+1)\Gamma(q)} \left(\frac{\rho}{\rho + q\lambda}\right)^k \left(\frac{q\lambda}{\rho + q\lambda}\right)^q, \end{aligned} \tag{2}$$

where $\Gamma(q)$ is the gamma function. From (2), we can see that K follows a Negative Binomial distribution [8], i.e., $K \sim NB(q, \frac{\rho}{\rho + q\lambda})$. As discussed in above, we consider that a BS with $K = 0$ is not active, which would be ignored in our analysis due to its muted transmission.

B. Wireless System Model

The two-dimensional (2D) distance between an arbitrary UE and an arbitrary BS is denoted by r. With regard to path loss modeling, we adopt a general and practical piece-wise path loss model with respect to r proposed in [9], where each piece of the path loss function is modeled as either a LoS transmission or a NLoS one. Such path loss function is given by

$$\zeta_{jlk}(r) = \begin{cases} \zeta_{1(jlk)}(r), & \text{when } 0 \leq r \leq d_1 \\ \zeta_{2(jlk)}(r), & \text{when } d_1 < r \leq d_2 \\ \vdots & \vdots \\ \zeta_{N(jlk)}(r), & \text{when } r > d_{N-1} \end{cases}, \tag{3}$$

where $\zeta_{n(jlk)}$ is the n-th piece of the path loss function between the j-th BS and the k-th UE scheduled by the l-th BS. Moreover, each piece of path loss function is modeled by

$$\zeta_n(r) = \begin{cases} \zeta_n^{\mathrm{L}}(r) = A_n^{\mathrm{L}} r^{-\alpha_n^{\mathrm{L}}}, & \text{LoS: } \Pr_n^{\mathrm{L}}(r) \\ \zeta_n^{\mathrm{NL}}(r) = A_n^{\mathrm{NL}} r^{-\alpha_n^{\mathrm{NL}}}, & \text{NLoS: } \Pr_n^{\mathrm{NL}}(r) \end{cases}, \tag{4}$$

where

- $\zeta_n^{\mathrm{L}}(r)$ and $\zeta_n^{\mathrm{NL}}(r), n \in \{1, 2, \ldots, N\}$ are the n-th piece path loss functions for the LoS and the NLoS cases, respectively,
- A_n^{L} and A_n^{NL} are the path losses at a reference 2D distance $r = 1$ for the LoS and the NLoS cases, respectively, α_n^{L} and α_n^{NL} are the path loss exponents for the LoS and the NLoS cases, respectively.
- $\Pr_n^{\mathrm{L}}(r)$ and $\Pr_n^{\mathrm{NL}}(r)$ are the n-th piece wise probability function that a transmission between an arbitrary UE and an arbitrary BS is a LoS path and a NLoS path, respectively. Note that $\sum_{n=1}^{N} \left(\Pr_n^{\mathrm{L}}(r) + \Pr_n^{\mathrm{NL}}(r)\right) = 1$.

Based on these path loss and probabilistic LoS/NLoS models, a practical UE association strategy (UAS) is considered in this paper. A UE is associated with the BS that provides the maximum average received signal strength (i.e. the largest $\zeta(r)$). Moreover, we assume that one *M*-antenna BS can at most simultaneously schedule K_{T} UEs in a time-frequency resource block.

For convenience, we denote a UE in each BS by the index of its used pilot sequence, i.e., the k-th UE is the UE that uses the k-th pilot sequence t_k, where k is randomly chosen from 1 to the maximum pilot sequence index K_{T}. Note that the k-th UE could be an empty UE, since not all of the pilot sequences are used at all time by each BS. If there are more than K_{T} UEs connected to a BS, only up to K_{T} of them are randomly chosen to be scheduled, which means that this BS is fully loaded and K_{T} pilot sequences are used. Without loss of generality and as mentioned earlier, we consider the first UE in B_1 as the typical UE, denoted by U_1, which is using the first pilot sequence.

Based on the above discussion, we focus on the active BSs and scheduled UEs and further study the distribution of the scheduled UE number per active BS, which can be denoted by a positive RV $\tilde{K}$. Considering (2) and the fact that the difference between K and $\tilde{K}$ lies in $\tilde{K} \neq 0$ and $\tilde{K} \leq K_{\mathrm{T}}$, we can conclude that $\tilde{K}$ follows a truncated Negative Binomial distribution with a PMF given by

$$f_{\tilde{K}}(\tilde{k}) = Pr[\tilde{K} = \tilde{k}] = \begin{cases} \frac{f_K(k)}{1 - f_K(0)}, & 1 \leq k \leq K_{\mathrm{T}} - 1 \\ \frac{\sum_{k=K_{\mathrm{T}}}^{\infty} f_K(k)}{1 - f_K(k)} & k = K_{\mathrm{T}} \end{cases}, \tag{5}$$

where $1-f_K(k)$ represents the probability that a BS is active and $\sum_{k=K_{\mathrm{T}}}^{\infty} f_K(k)$ represents the probability that a BS is fully loaded with K_{T} scheduled UEs.

C. Pilot-Aided mMIMO Channel Estimation

In this paper, the channel is assumed to be invariant in a time-frequency resource block, and change independently from block to block. The channel is then modeled as

$$\mathbf{h}_{jlk} = (\zeta_{jlk})^{\frac{1}{2}} \Phi_{jlk}^{\frac{1}{2}} \mathbf{w}_{jlk}, \tag{6}$$

where $\mathbf{h}_{jlk}$ is the channel vector between the j-th BS and the k-th UE scheduled by the l-th BS, $\mathbf{w}_{jlk}$ is the multi-path fading vector modeled according to Rayleigh fading, and Φ_{jlk} is the co-variance matrix of the channel.

Moreover, the UL transmit power is assumed to follow a distance-dependent fractional power compensation scheme, and is modeled as

$$P_{lk}^{\mathrm{tx}} = P_{\mathrm{UE}}^{\mathrm{tx}} (\zeta_{llk}(r))^{-\epsilon}, \tag{7}$$

where P_{lk}^{tx} is the transmit power from the k-th UE scheduled by the l-th BS, $P_{\mathrm{UE}}^{\mathrm{tx}}$ is the baseline transmit power of the UE, and $\epsilon \in [0,1]$ is the fraction of the path loss compensation.

In the UL training stage, pilot contamination is considered, and thus the channel $\mathbf{y}_{11}$ observed at BS B_1 for the typical UE U_1 is given by

$$\mathbf{y}_{11} = \sqrt{P_{11}^{\mathrm{tx}}} \mathbf{h}_{111} + \sum_{l \neq 1} \sqrt{P_{1l}^{\mathrm{tx}}} \mathbf{h}_{1l1} + \mathbf{n}_1, \tag{8}$$

where the l-th neighbouring BS also schedules an interfering UE using the first pilot sequence, and $\mathbf{n}_1$ denotes a zero-mean additive white Gaussian noise (AWGN) vector at the typical UE U_1, where the variance of each element is σ^2. Note that the first pilot sequence may not be used by all BSs.

From the observation of the pilot signals transmitted from UEs, BSs can estimate their channels by correlating the corresponding pilot sequences with the observation by using an MMSE estimator. Since the channel $\mathbf{h}_{111}$ is modeled as i.i.d. Rayleigh fading, the estimated channel $\bar{\mathbf{h}}_{111}$ can be calculated as

$$\bar{\mathbf{h}}_{111} = \frac{\sqrt{P_{11}^{\mathrm{tx}}} \zeta_{111}}{\sum_{l \neq 1} P_{l1} \zeta_{1l1} + \sigma^2} \mathbf{y}_{11}. \tag{9}$$

The estimate error can then be computed by $\hat{\mathbf{h}}_{111} = \mathbf{h}_{111} - \bar{\mathbf{h}}_{111}$.

D. Performance Metrics

In the UL data transmission stage, we assume that the BSs apply the maximum ratio combining (MRC) receiver based on the estimated channel obtained in the UL training stage. Note that there can be LoS or NLoS transmission between the typical UE and the typical BS. We take the LoS case as an example to show our analysis. The UL SINR of the typical UE with a LoS transmission is given by

$$\mathrm{SINR} = \frac{P_{11}^{\mathrm{tx}} \left| \mathbf{g}_{11}^{\mathrm{H}} \bar{\mathbf{h}}_{111} \right|^2}{P_{11}^{\mathrm{tx}} \left| \mathbf{g}_{11}^{\mathrm{H}} \hat{\mathbf{h}}_{111} \right|^2 + \sum_{(l,k) \neq (1,1)} P_{lk}^{\mathrm{tx}} \left| \mathbf{g}_{11}^{\mathrm{H}} \mathbf{h}_{1lk} \right|^2 + \left| \mathbf{g}_{11}^{\mathrm{H}} \right|^2 \sigma^2}, \tag{10}$$

where $\mathbf{g}_{11}$ is the combining vector employed at B_1 for the typical UE U_1 with LoS transmission, and the result is derived by assuming that the uplink data symbols for the k-th UE in the l-th BS s_{lk} satisfies $\mathbf{E}\left[|\mathrm{s_{lk}}|^2\right] = 1$. Note that the NLoS transmission between the typical UE and the typical BS has a similar expression, which is omitted here for brevity. We take the LoS transmission as an example to show our analysis. Using the SINR expression in (10), the coverage probability $p^{\mathrm{cov}}(\lambda, \rho, \gamma)$ can be defined as $p^{\mathrm{cov}} = \Pr(\mathrm{SINR} > \gamma)$, where γ is a SINR threshold. The sum spectral efficiency in BS B_1 in bps/Hz/BS can be computed as

$$R_1 = \sum_{\tilde{k}=1}^{K_{\mathrm{T}}} \tilde{k} \, f_{\tilde{K}}(\tilde{k}) \int_{\gamma_0}^{\infty} \log_2(1+\gamma) f_{\Gamma}(\lambda, \rho, \gamma) d\gamma, \tag{11}$$

where $f_{\Gamma}(\lambda, \rho, \gamma)$ is the probability density function (PDF) of the uplink SINR at the typical BS B_1, which can be written as

$$f_{\Gamma}(\lambda, \rho, \gamma) = \frac{\partial (1 - p^{\mathrm{cov}}(\lambda, \rho, \gamma))}{\partial \gamma}. \tag{12}$$

Following the definition in [10], we compute the area spectral efficiency (ASE) in bps/Hz/km^2 by multiplying the sum spectral efficiency per BS with the active BS density as

$$A^{\mathrm{ASE}}(\lambda, \rho, \gamma_0) = \tilde{\lambda} R_1. \tag{13}$$

III. Analysis Based On the Proposed system model

The main goal of this section is to present our theoretical results on network performance.

A. Coverage Probability Analysis

To conduct a relatively tractable study of the coverage probability performance, we make the following assumption.

Assumption1. The scheduled UEs using the same pilot sequence e.g. the k-th pilot sequence are modeled as a HPPP Φ_k with a density $\lambda^k = \tilde{\lambda}(\frac{\sum_{\tilde{k}=1}^{K_{\mathrm{T}}} \tilde{k} f_{\tilde{K}}(\tilde{k})}{K_{\mathrm{T}}})$, and the scheduled UEs using a different pilot sequence are assumed to be independently distributed.

Proof: See Appendix A ∎

Previously, we have defined coverage probability $p^{\mathrm{cov}}(\lambda, \rho, \gamma)$ as the probability that the SINR is larger than a threshold γ. Based on the presented system models and Assumption 1, we can analyze $p^{\mathrm{cov}}(\lambda, \rho, \gamma)$ using the following theorem.

Theorem 1. *$p^{cov}(\lambda, \rho, \gamma)$ can be computed as*

$$p^{cov}(\lambda, \rho, \gamma) = \sum_{n=1}^{N} (T_n^{\mathrm{L}} + T_n^{\mathrm{NL}}), \tag{14}$$

where

$$T_n^{\mathrm{L}} = \int_{d_{n-1}}^{d_n} \sum_{m=1}^{M} \binom{N}{m} (-1)^{m+1} e^{(-m\gamma\{\mathrm{SINR}_n^L\}^{-1})} f_n^L(r) dr, \quad (15)$$

$$T_n^{\mathrm{NL}} = \int_{d_{n-1}}^{d_n} \sum_{m=1}^{M} \binom{N}{m} (-1)^{m+1} e^{(-m\eta\gamma\{\mathrm{SINR}_n^{NL}\}^{-1})} f_n^{NL}(r) dr, \quad (16)$$

where $\eta = N(N!)^{-\frac{1}{N}}$ *and* d_n *is defined in (3).* r *is the distance between the typical UE* U_1 *and the typical BS* B_1*. Moreover,* $f_n^L(r)$ *and* $f_n^{NL}(r)$ *are computed by*

$$f_n^{\mathrm{L}}(r) = Pr^{\mathrm{L}}(r) 2\pi r\lambda \exp(-\int_0^r Pr^{\mathrm{L}}(u) 2\pi u\lambda du) \times \exp(-\int_0^{r_1} Pr^{\mathrm{NL}}(u) 2\pi u\lambda) du, \quad (d_{n-1} < r < d_n), \quad (17)$$

and

$$f_n^{\mathrm{NL}}(r) = Pr^{\mathrm{NL}}(r) 2\pi r\lambda \exp(-\int_0^r Pr^{\mathrm{NL}}(u) 2\pi u\lambda du) \times \exp(-\int_0^{r_2} Pr^{\mathrm{L}}(u) 2\pi u\lambda) du, \quad (d_{n-1} < r < d_n), \quad (18)$$

where r_1 *and* r_2 *are given implicitly by the following equations:* $r_1 = \arg\limits_{r_1} \left\{\zeta^{\mathrm{NL}}(r_1) = \zeta_n^{\mathrm{L}}(r)\right\}$ *and* $r_2 = \arg\limits_{r_2} \left\{\zeta^{\mathrm{L}}(r_2) = \zeta_n^{\mathrm{NL}}(r)\right\}$.

Proof: See Appendix B ∎

As a special case to show our analytical results in the following sections, we consider a practical two-piece path loss function and a two-piece linear LoS probability function, defined by the 3GPP [11]. Specifically, we have $N = 2$, $\zeta_1^{\mathrm{L}}(r) = \zeta_2^{\mathrm{L}}(r) = A^{\mathrm{L}} r^{-\alpha^{\mathrm{L}}}$, $\zeta_1^{\mathrm{NL}}(r) = \zeta_2^{\mathrm{NL}}(r) = A^{\mathrm{NL}} r^{-\alpha^{\mathrm{NL}}}$, $\mathrm{Pr}_1^{\mathrm{L}}(w) = 1 - \frac{r}{d_1}$, and $\mathrm{Pr}_2^{\mathrm{L}}(w) = 1$, where $d_1 = 300$ m [11]. For clarity, this case is referred to as **the 3GPP Case** hereafter. According to 1, $p^{\mathrm{cov}}(\lambda, \rho, \gamma)$ can be computed by

$$p^{\mathrm{cov}}(\lambda, \rho, \gamma) = \sum_{n=1}^{2} (T_n^{\mathrm{L}} + T_n^{\mathrm{NL}}). \quad (19)$$

IV. Results and Discussion

In this section, we present numerical results to validate the accuracy of our analysis and further study the capacity performance of UL mMIMO networks. In this section. According to Tables A.1-3~A.1-7 of [11], we adopt the following parameters for the 3GPP Case: $\alpha^{\mathrm{L}} = 2.09$, $\alpha^{\mathrm{NL}} = 3.75$, $A^{\mathrm{L}} = 10^{-10.38}$, $A^{\mathrm{NL}} = 10^{-14.54}$, $\mathrm{P}_{\mathrm{UE}}^{\mathrm{tx}} = -76$ dBm and a noise figure of 9 dB at each dB.

A. Coverage Probability Performance

In this subsection, we first validate the analytical results of the coverage probability, considering a network deployment with a BS density λ=10 BSs/km^2, and presenting results for several combinations of UE densities ρ, number of antennas per BS M, maximum number of scheduled UE per BS K_{T}, and fraction of the path loss compensation in the UL power control ϵ.

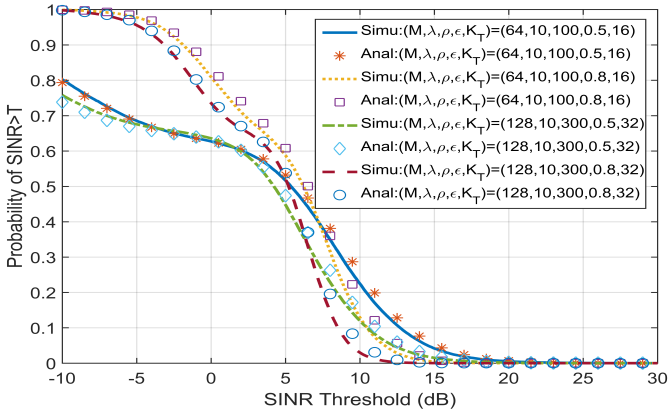

Fig. 1. The coverage probability $p^{\mathrm{cov}}(\lambda, \rho, \gamma)$ vs. the SINR threshold with $\lambda = 10$ BSs/km^2. The Analytical results drawn based on theorem 1 match well with simulation.

From Fig. 1, we can see that the analytical results fit well with the simulation ones for the wide variety of studied cases. This validates our theoretical modeling.

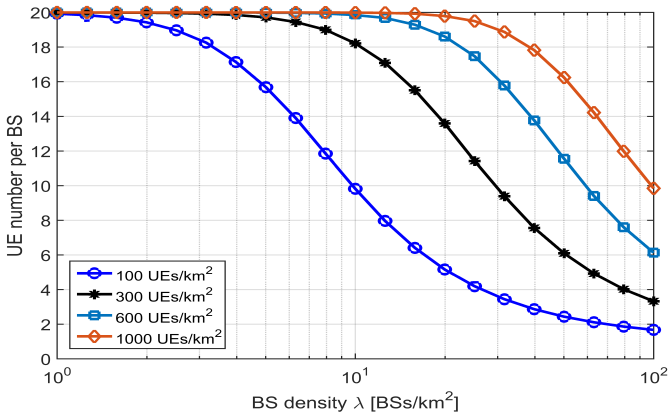

Fig. 2. Scheduled UE number per BS vs BS density λ with different UE density ρ

In the following, we study in more detail the coverage probability, as a function of the BS density. However, before doing that, in Fig. 2, we plot the average number of scheduled UEs per BS as a function of the BS density λ for various values of the UE density ρ with M =64, ϵ =0.8 and K_{T} =20. From Fig. 2, we can see that the average number of scheduled UEs per BS decreases as λ increases for all values of ρ.

With this results in mind, in Fig. 3, we study the coverage probability as a function of the BS density. The same parameters as in Fig. 2 are used. From Fig. 3, we can see that:

- When the BS density is relatively small, e.g., $\lambda \in [1, 4]$ BSs/km^2, the coverage probability performance of all UE densities are similar. In this BS density range, the coverage probability curves first decrease, and then increase. The intuition behind this trend is that when the BS density is much smaller compared with the UE density, every

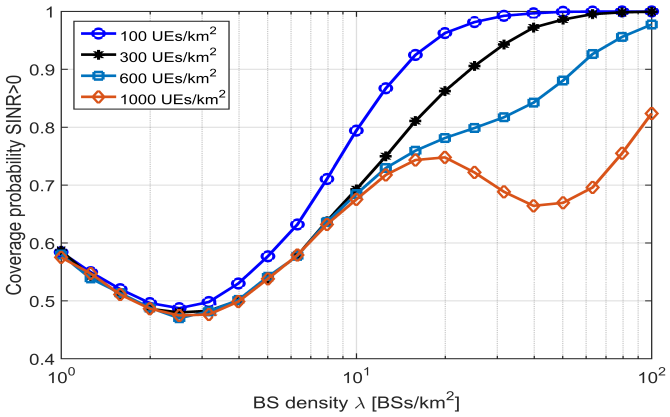

Fig. 3. The coverage probability $p^{\text{cov}}(\lambda, \rho, \gamma)$ vs. the BS density λ with $M = 64$, $\epsilon = 0.8$ and $K_{\text{T}} = 20$. Different UE denisties are considered in this network deployment.

newly-added BS is likely to be fully loaded by scheduling the maximum number of UEs. When we go from 1 BS to 2.5 BSs per km^2, we move from a noise limited to an interference limited scenario, and thus the received interference power in both the training and data phase grows faster than the signal power. As consequence, the SINR and thus the coverage probability decrease. Once we have more than 2.5 BSs per km^2, the interference starts growing at a lower pace than before, and the network benefits from the closer proximity between a UE and its server, i.e. a stronger carrier signal. As a result, the coverage probability increases.

- When the BS density increases beyond 4 BSs/km^2, and the UE density is small, a higher BS density always results in a higher coverage probability because the signal power grows stronger and stronger, transiting from NLoS to LoS, but also because *i)* the interference power decreases due to the UL power control and *ii)* the less pilot contamination since cells are less loaded as shown in Fig. 3 and thus are more unused pilot sequences. However, when the UE density is large, e.g. ρ=1000 UEs/km^2, the coverage probability first decreases (when the BS density is λ=15 BSs/km^2), and then increases (when the BS density is λ=40 BSs/km^2). The intuition behind this interesting behavior is the following. When the BS density increases above a threshold, the interfering UEs become closer and closer to the serving BSs, and some interference signals transition from NLoS to LoS. Due to this transition, the received interference power in both the training and data phase grows again faster than the signal power. As consequence, the SINR and thus the coverage probability decrease again. Note that this impact is reduced with a lower UE density. For example, we can see that when ρ=600 UEs/km^2, the mentioned decrease and increase is milder due to the less interfering paths transitioning from NLoS to LoS.
- Note that regardless of the UE density, the coverage probability $p^{\text{cov}}(\lambda, \rho, \gamma)$ always increases with the BS density when such density is sufficiently large, e.g., $\lambda > 40$ BSs/km^2. The reason is the BS idle mode capability. Under this consideration, the signal power continues increasing with the network densification, while the interference power significantly decreases due to the UL power control. Moreover, pilot contamination is also significantly lower since very few pilot sequences are used per BS when the BS density is large.

B. Network Capacity performance

In this subsection, we further investigate the network capacity, and explain how the UE density and BS density impact the ASE performance.

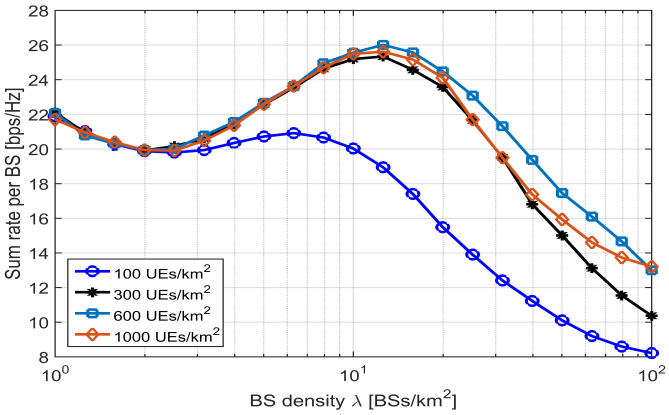

Fig. 4. The sum spectral efficiency per BS R_1 vs. BS density λ with $\gamma_0 = 0$ and different UE density ρ

In Fig. 4, we plot the sum spectral efficiency per BS R_1 with $\gamma_0 = 0$ as a function of the BS density λ for various values of the UE density ρ. From Fig. 4, we observe that similar as for the coverage probability, the sum spectral efficiency per BS first decreases when we move from a noise limited to an interference limited scenario. Then, it increases when the network becomes denser, and thus the signal power gets stronger due to the closer proximity of UEs and BSs, the interference power get weaker due to the UL power control. Finally, the sum spectral efficiency per BS decreases again when the number of UEs per BS starts to significantly decreases, as shown in Fig. 3.

According to (13), ASE is computed by multiplying R_1 and $\tilde{\lambda}$. In Fig. 5, we plot the ASE vs. BS density with $\gamma_0 = 0$ and various UE density and predicate the ASE performance with large BS density. From Fig. 5, we can conclude that a larger BS density always results in a higher ASE. When the BS density is small, the ASE performance quickly increases almost linearly with the BS density λ due to the dramatic increase of the number of scheduled UE per BS despite of the initial decrease of the coverage probability. When λ is large enough for different ρ, e.g. $\lambda > 15$ BSs/km^2 with $\rho = 100$ UEs/km^2, the ASE growth rate slows down. Such slow down behavior indicates that since the UE density is finite, at some point, densifying further those not introduce more spatial reuse but increases the inter-cell interference. However, it is

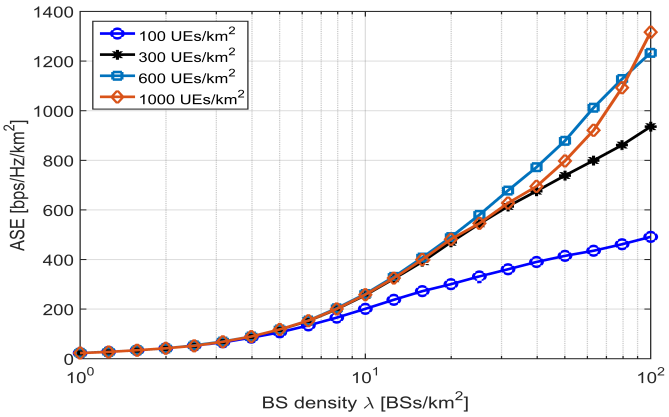

Fig. 5. The ASE $ASE(\lambda, \rho, \gamma_0)$ with $\lambda = 10\,\text{BSs/km}^2$ and $\gamma_0 = 0\,\text{dB}$ vs BS density λ with different UE densities

important to note that it is unrealistic to have that large BS density like 100 BSs/km^2 in mMIMO networks.

Moreover, for a given λ, e.g. λ =30 BSs/km^2, we can see that the ASE is also a concave function of the UE density ρ, and its maximum value lies in $\rho \in [300, 1000]$ UEs/km^2, which is logically correct from the conclusion of performance decline in coverage probability and sum rate per BS observed at such BS density.

V. Conclusions

In this paper, we have conducted a performance analysis of UL mMIMO network with LoS and NLoS transmission and finite UE density. Approximate analytical results were derived for the coverage probability and ASE. Based on our results, the performance impact of LoS/NLoS and finite UE density is shown to be significant. Specifically, we found that *(i)* the coverage probability may suffer from a slow growth or decrease as BS density increases; *(ii)* there should be an optimal BS density to maximum the sum rate per BS for a given UE density; *(iii)* however, the ASE performance keeps increasing with the BS density. For future work, we will further study the optimal ASE performance with considerations of different factors and performance impacts of other factors such as maximum scheduled UE number per BS and ZF receiver.

Appendix A: Proof of Assumption III-A

To prove Assumption 1, we need to compute the probability of the k-th UE is scheduled in the l-th BS:

$$\mathbf{1}(k_l) = \frac{k_{ave}}{K_{Total}}, \tag{20}$$

where k_{ave} is the average scheduled UE number per BS computed by: $k_{ave} = \sum_{k=1}^{K_{Total}} k f_{\hat{K}}(k)$.

Thus, we can approximate the desired BS density λ^{On*} as follows

$$\lambda^{On*} = \frac{E(\sum_{l\in\Phi_B} k_l)}{\lambda}\lambda^{On} = \frac{K_{ave}}{K_{Total}}\lambda^{On}. \tag{21}$$

Appendix B: Proof of Theorem 1

Due to page limitation, we defer the detailed proof to our journal version and provide brief explanation here.

In theorem 1, T_n^{L} and T_n^{NL} are the components of coverage probability responsible for the cases when typical BS and typical UE are connected with the n-th LoS path and with the n-th NLoS path respectively. We approximate $\mathrm{SINR}_n^{\mathrm{L}}$ by taking the expectation on each term using the properties of stochastic geometry and some basic algebraic operations:

$$\mathrm{SINR}_n^{\mathrm{L}} \approx \frac{(M+1)(\zeta_{01}^L)^{2(1-\epsilon)}}{\zeta_{01}^{L(1-\epsilon)}\left(\Lambda+\frac{\sigma^2}{P_t}\right)+\left(\zeta_{01}^{L(1-\epsilon)}+\Lambda\right)\left(\Delta_{PL}^{1-\varepsilon}+\sum_{k=1}^{K-1}k\Lambda f_{\tilde{K}}(\tilde{k})+\frac{\sigma^2}{P_t}\right)}, \tag{22}$$

where $\Delta_{PL}^{1-\varepsilon} = \sum_{k=1}^{K-1} k \int_0^\infty A_L r^{(\alpha_L\epsilon-1)} f_n^L(r) dr f_{\tilde{K}}(\tilde{k})$ and $\Lambda = \int_r^\infty A_{PL} x^{\alpha_{PL}} \mathbb{E}\left(\left(\zeta_{llk}^{PL}\right)^{-\epsilon}\right) 2\pi x \lambda^k P r^{PL}(x) dx$.

Since SINR expression is considered as a function of the distance between typical UE and typical BS r, the CCDF of SINR is $P(SINR_L(r) > T)$ where T is the SINR threshold. Following [4], we use a gamma distribution to approximate the distribution of SINR as follows:

$$P(SINR_L(r) > T) = P(1 > \tfrac{T}{SINR_L(r)}) \approx P(g > \tfrac{T}{SINR_L(r)}) \approx \sum_{m=1}^{N} \binom{n}{N} (-1)^{n+1} e^{-nN(N!)^{-\frac{1}{N}} T SINR_L(r)} = T_n^{\mathrm{L}}. \tag{23}$$

Since the derivation of T_n^{NL} is very similar with that of T_n^{L}, it is omitted for brevity. Our proof is completed with applying T_n^{NL} and T_n^{L} in (14).

References

[1] E. G. Larsson, O. Edfors, F. Tufvesson, and T. L. Marzetta, "Massive mimo for next generation wireless systems," *IEEE Communications Magazine*, vol. 52, no. 2, pp. 186–195, February 2014.

[2] T. L. Marzetta, "Noncooperative cellular wireless with unlimited numbers of base station antennas," *IEEE Transactions on Wireless Communications*, vol. 9, no. 11, pp. 3590–3600, November 2010.

[3] N. Krishnan, R. D. Yates, and N. B. Mandayam, "Uplink linear receivers for multi-cell multiuser mimo with pilot contamination: Large system analysis," *IEEE Transactions on Wireless Communications*, vol. 13, no. 8, pp. 4360–4373, Aug 2014.

[4] T. Bai and R. W. Heath, "Analyzing uplink sinr and rate in massive mimo systems using stochastic geometry," *IEEE Transactions on Communications*, vol. 64, no. 11, pp. 4592–4606, Nov 2016.

[5] D. Lopez-Perez, M. Ding, H. Claussen, and A. H. Jafari, "Towards 1 gbps/ue in cellular systems: Understanding ultra-dense small cell deployments," *IEEE Communications Surveys Tutorials*, vol. 17, no. 4, pp. 2078–2101, Fourthquarter 2015.

[6] M. Ding, D. L. Perez, G. Mao, and Z. Lin, "Study on the idle mode capability with los and nlos transmissions," in *2016 IEEE Global Communications Conference (GLOBECOM)*, Dec 2016, pp. 1–6.

[7] M. Ding, D. López-Pérez, G. Mao, and Z. Lin, "What is the true value of dynamic TDD: A MAC layer perspective," *to appear in Globecom 2017, arXiv:1611.02828 [cs.NI]*, Mar. 2017.

[8] I. S. Gradshteyn and I. M. Ryzhik, *Table of integrals, series, and products*. Academic press, 2014.

[9] M. Ding, D. López-Pérez, G. Mao, and Z. Lin, "Performance impact of idle mode capability on dense small cell networks with LoS and NLoS transmissions," *to appear in IEEE Transactions on Vehicular Technology, arXiv:1609.07710 [cs.NI]*, Mar. 2017.

[10] M. Ding, D. Lopez-Perez, G. Mao, P. Wang, and Z. Lin, "Will the area spectral efficiency monotonically grow as small cells go dense?" *IEEE GLOBECOM 2015*, pp. 1–7, Dec. 2015.

[11] 3GPP, "TR 36.828: Further enhancements to LTE Time Division Duplex for Downlink-Uplink interference management and traffic adaptation," Jun. 2012.